PHYSICAL REVIEW B, VOLUME 63, 064106

Pressure-induced phase transitions in chromium thiospinels

P. Vaqueiro and A. V. Powell
Department of Chemistry, Heriot-Watt University, Edinburgh EH14 4AS, United Kingdom

S. Hull and D. A. Keen
Rutherford Appleton Laboratory, ISIS Facility, Didcot, Oxfordshire OX11 0QX, United Kingdom

(Received 28 August 2000; published 23 January 2001)

The pressure and temperature dependence of the structure of $CoCr_2S_4$ and $Co_{0.65}Ni_{0.35}Cr_2S_4$ have been studied by *in situ* time-of-flight powder neutron diffraction. While the thiospinel $CoCr_2S_4$ transforms to a defect NiAs-type phase at 1.3 GPa and 800 °C, the nickel-doped thiospinel undergoes this phase change at 0.4 GPa and 750 °C. Quenching of the hexagonal high-temperature and high-pressure phase resulted in a transition to a monoclinic Cr_3S_4 phase, due to the ordering of the metal vacancies in every second layer. Moreover, the spinel $CoCr_2S_4$ transforms at room temperature and 8.6 GPa to a phase which does not exhibit a NiAs-type structure.

DOI: 10.1103/PhysRevB.63.064106 PACS number(s): 61.50.Ks, 64.70.Kb

I. INTRODUCTION

Materials of general formula ACr_2X_4 in which A is a transition metal and $X=O$, S, Se, or Te, adopt either the spinel[1] or a defect NiAs-type structure.[2] For $X=O$, only the spinel structure is found, while for $X=$ Se or Te a defect NiAs-type structure is favored. In contrast to this, for $X=S$ both structures may be found, depending on the nature of A. When $A=$ Mn, Fe, Co, Cu, materials adopt the spinel structure, while materials with $A=$ Ti, V, Cr, Ni have a defect NiAs-type structure. This implies that for the ternary sulphides, the difference in energy between the two forms is small.

The spinel[3] and the NiAs (Ref. 4) structures differ in the stacking sequence of the anions, which is cubic for the spinel and hexagonal for the NiAs structure, and in the coordination of the cations. In the spinel structure 1/3 of the cations reside at tetrahedral sites and the other cations are octahedrally coordinated, whereas in the NiAs structure all cations reside at octahedral sites. The latter form therefore has a higher density, and hence thiospinels should undergo a phase transition to a defect NiAs-type phase under pressure. It has been shown that heating ACr_2S_4 ($A=$ Mn, Fe, Co) spinels at elevated temperatures and pressures allows isolation of defect NiAs-type phases by rapid quenching.[5–8] In these studies, two high-pressure NiAs-type phases have been isolated: a cation-deficient NiAs phase, with hexagonal symmetry, and a monoclinic Cr_3S_4 phase. These two structures are closely related; in the Cr_3S_4 structure the cation vacancies are ordered and confined to every second layer along the c axis, while in the cation-deficient NiAs phase the vacancies are disordered and distributed randomly in every layer (Fig. 1). It has been suggested that high pressures favor the ordered Cr_3S_4 phase, while at lower pressures the disordered cation-deficient NiAs phase is formed.[7] However, a transformation to the higher symmetry NiAs phase at high temperatures has been observed for materials which adopt the Cr_3S_4 structure at ambient temperature.[4,9] The structural transformation from thiospinel to a NiAs-type phase is accompanied by a semiconductor-to-metal transition[10] as well as by changes in magnetic properties.[11]

We sought to investigate pressure and temperature induced structural changes in the thiospinel $CoCr_2S_4$, by *in situ* powder neutron diffraction. Furthermore, in an effort to lower the temperature and pressure required to effect the structural transformation, and hence the metal-insulator transition, partial replacement of cobalt by nickel has been investigated. We have previously reported the preparation, characterization and physical properties of materials in the

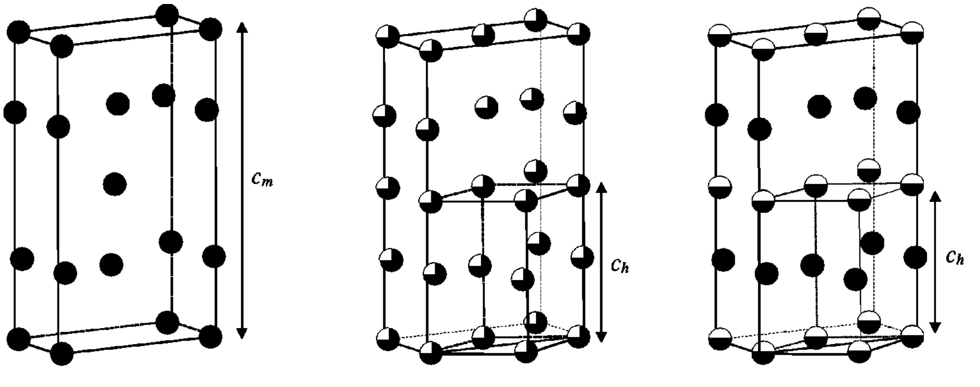

FIG. 1. Relationship between (a) the Cr_3S_4 structure, (b) the cation-deficient NiAs structure, and (c) the CdI_2 structure. Anions are omitted for clarity. Black circles represent fully occupied cation sites, half black circles represent a site occupancy of 0.5, and three quarter black circles represent a site occupancy of 0.75.

series $Co_{1-x}Ni_xCr_2S_4$.[12] Results demonstrate that the single-phase region of spinel type extends over the composition range $0 \leqslant x \leqslant 0.35$. Here, we compare the behavior under pressure and temperature of the end member $CoCr_2S_4$ with the nickel doped material $Co_{0.65}Ni_{0.35}Cr_2S_4$, which is close to the limit of stability for the spinel structure. We also present the behavior of $CoCr_2S_4$ at room temperature under very high pressures (up to 10 GPa).

II. EXPERIMENT

$CoCr_2S_4$ and $Co_{0.65}Ni_{0.35}Cr_2S_4$ were synthesized from the elements at elevated temperatures. Mixtures of cobalt (Strem Chemicals, 99.8%), nickel (Aldrich, 99.99%), chromium (Aldrich, 99+%), and sulphur (Aldrich, 99.98%) with the appropriate stochiometry were ground in an agate mortar prior to sealing into evacuated ($\leqslant 10^{-4}$ torr) silica tubes. Mixtures were fired at 800–1000 °C for a period of between 7 and 13 days with intermediate regrinding. Samples were cooled at 4 °C/min to 300 °C prior to removal from the furnace. Details of the preparation and characterization have been presented elsewhere.[12]

Time-of-flight powder neutron-diffraction data were collected on the Polaris diffractometer at ISIS, Rutherford Appleton Laboratory. *In situ* high-temperature, high-pressure data were collected using a high temperature version of the McWhan clamped cell, developed at ISIS,[13] and capable of achieving 800 °C and 1.3 GPa. This cell incorporates a thin tubular graphite heating element around the sample can and an integral hydraulic ram, which drives tungsten carbide anvils to generate pressure on the sample. Boron nitride collimation gives powder-diffraction patterns without background from the cell when using the 90° bank of detectors. The sample was precompressed into a platinum can prior to mounting in the cell and no pressure calibrant was added. The sample pressure and temperature were determined by calibration of the cell with NaCl.[13] It was not possible to add a pressure transmitting fluid, since the liquid would evaporate or decompose at high temperature. During the course of the experiment, reflections arising from the lid of the platinum can, appeared in the diffraction patterns, owing to the significant reduction in volume of the sample. Gd foil was thus used to reduce the cell window size and eliminate these Pt reflections. *In situ* room-temperature high-pressure data were collected using the Paris-Edinburgh clamped cell[14] over the applied pressure range $0 < P/\mathrm{GPa} \leqslant 10$. In this cell, the sample volume ($\sim 100\ \mathrm{mm}^3$) is formed by the hole in a TiZr alloy gasket and central indentations in the anvil faces. Owing to the small sample volume, long data collection times (~8 h) were required. Fluorinert was added to the sample as a pressure transmitting medium and no pressure calibrant was used. On the basis of previous measurements carried out on this cell, the sample pressure is estimated to be 90% of the applied pressure. Initial data manipulation and reduction was carried out using Genie spectrum manipulation software.[15] Spectra were corrected for the effects of wavelength-dependent attenuation due to the cell. Neutron-diffraction data, from the 90° bank of detectors were summed and normalized for subsequent use in Rietveld refinement using the GSAS package.[16] In all refinements, the neutron background was described by a polynomial and the peak shape by a convolution of an exponential and a pseudo-Voigt function. The background and peak shape coefficients were included as refinable parameters. A sample-absorption parameter was also included, using the Debye-Scherrer absorption correction model. In all refinements, site occupancy factors (SOF) were fixed at the nominal composition and an overall thermal parameter was refined.

Magnetic measurements were performed using a Quantum Design MPMS2 superconducting quantum interference device susceptometer. Samples were loaded into gelatin capsules at room temperature and data were collected over the temperature range $5 \leqslant T/\mathrm{K} \leqslant 300$, after cooling in the measuring field of 1000 G. Data were corrected for the diamagnetism of the gelatin capsule.

TABLE I. Final refined atomic parameters for $CoCr_2S_4$ at 1.3 GPa and 800 °C (CdI_2 phase, space group: $P\overline{3}m1$), with refined lattice parameters: $a = 3.4319(2)$ Å and $c = 5.5836(9)$ Å. The final goodness-of-fit indicators are $R_{wp} = 12.8\%$ and $\chi^2 = 1.0$, and the refined weight fraction for the CdI_2 phase is 76%.

Atom	Site	x	y	z	B (Å^2)	SOF
Co	1(a)	0.0	0.0	0.0	1.7(1)	0.5
Cr	1(b)	0.0	0.0	0.5	1.7(1)	1.0
S	2(d)	1/3	2/3	0.251(4)	1.7(1)	1.0

III. RESULTS

A. High-temperature and high-pressure study on $CoCr_2S_4$

Data were collected, under an applied pressure of 1.3 GPa, over the temperature range $25 \leqslant T/°\mathrm{C} \leqslant 800$. Over the temperature range $25 \leqslant T/°\mathrm{C} \leqslant 650$ all reflections in the diffraction patterns can be assigned to a spinel phase, although at 650 °C some additional reflections, originating from the lid of the platinum can, can also be observed. At 800 °C, the highest temperature achievable with this cell, the spinel reflections decrease markedly in intensity, and new peaks, which can be indexed on the basis of a hexagonal CdI_2 unit cell, appear. The structure of the cation-rich CdI_2 is very similar to that of the cation-deficient NiAs (Fig. 1). While in the latter structure vacancies are distributed randomly between all layers, in the CdI_2 structure fully occupied layers alternate with half occupied layers, in which vacancies are disordered. Using the data collected at 800 °C, a three-phase Rietveld refinement was carried out. In this refinement, the Pt phase was refined using the structure-independent Le Bail method,[17] while the spinel and the CdI_2 phases were refined in the usual way. Final refined parameters for data collected at 800 °C are given in Table I and the final observed, calculated and difference profiles are presented in Fig. 2. Cooling of the cell to room temperature resulted in a reversible transformation of the CdI_2 phase to the spinel phase.

B. High-temperature and high-pressure study on $Co_{0.65}Ni_{0.35}Cr_2S_4$

Data were collected, under an applied pressure of 0.4 GPa, over the temperature range $25 \leqslant T/°\mathrm{C} \leqslant 750$. Above

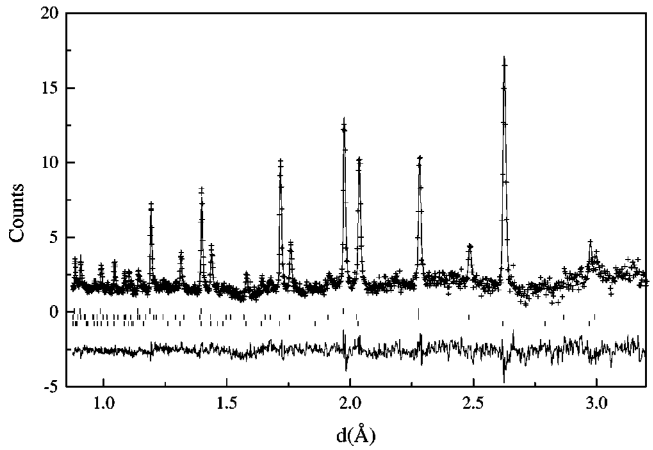

FIG. 2. Observed (crosses), calculated (upper full line) and difference (lower full line) powder neutron-diffraction profiles for $CoCr_2S_4$ at 1.3 GPa and 800 °C. Lower markers correspond to reflections of the CdI_2 phase, middle markers are for the spinel phase and upper markers for the Pt phase.

420 °C some additional reflections, arising from the lid of the platinum can, are observed. At 650 °C, the spinel reflections decrease in intensity, and new peaks, which can be indexed on the basis of a cation-deficient NiAs unit cell, appear. At 750 °C, only the reflections assigned to the new phase (NiAs) remain. Cooling of the sample to room temperature under pressure, over a 30-min period, did not result in a phase transition to the initial spinel, nor in the retention of the cation-deficient NiAs structure. The pattern collected after cooling under these conditions could be indexed on the basis of a monoclinic Cr_3S_4 unit cell, similar to that of $NiCr_2S_4$.[18]

Rietveld refinements using data collected below 750 °C were initiated with the structure determined for $Co_{0.65}Ni_{0.35}Cr_2S_4$ at room temperature and ambient pressure.[12] In refinements using data collected over the temperature range $420 \leqslant T/°C \leqslant 650$, a Pt phase was introduced. As before, this phase was refined using the Le Bail method. In the refinement using data collected at 650 °C, a NiAs-type phase was also included. Final refined parameters, together with selected bond lengths and angles for data collected below 750 °C are shown in Table II. With increasing temperature, the lattice parameter of the spinel increases, while the positional parameter u decreases, approaching its ideal value. In the spinel structure, the positional parameter u describes the deviation of the anions from the ideal fcc configuration. With the origin of coordinates chosen in this work, the ideal fcc configuration of the anion framework is given by a value of u of 0.25. For $u > 0.25$ the octahedra become distorted and as a consequence, the S-Cr-S angles diverge from the ideal value of 90°. Therefore, with increasing temperature, the octahedra approach their ideal cubic symmetry, while the A-S distances decrease and the Cr-S distances increase. This is reflected in the different behavior of the volume of the polyhedra. Whereas the volume of the octahedra increases by $>8\%$, the volume of the tetrahedra decreases by ca. 10%.

Before collecting data at 750 °C, the size of the cell windows was reduced using Gd foil, which proved to be an effective way of removing scattering from the lid of the Pt sample can. In the Rietveld refinement for data collected at 750 °C only a NiAs-type phase was included and a preferred orientation parameter was used. Although the refinement can be successfully carried out in the space group $P6_3/mmc$ (NiAs structure), refinements in the space group $P\bar{3}m1$, corresponding to a CdI_2 structure, resulted in similar values for the goodness-of-fit indicators. These two structures differ only in the distribution of the metal vacancies between layers (Fig. 1). In the experiment carried out on $CoCr_2S_4$, the high-pressure and high-temperature phase was identified as CdI_2 because of the presence of the (111) reflection ($d = 1.64$ Å), which is not allowed in the space group $P6_3/mmc$. However, in the simulation carried out for $Co_{0.65}Ni_{0.35}Cr_2S_4$ in the space group $P\bar{3}m1$, the (111) reflection has almost zero intensity and therefore a CdI_2 structure cannot be excluded.

TABLE II. Final refined parameters, selected bond lengths and angles for the spinel phase at 0.4 GPa as a function of temperature (space group: $Fd\bar{3}m$). Co atoms reside in the 8(a) site (1/8,1/8,1/8), Cr atoms in 16(d) (1/2,1/2,1/2), and sulphur atoms in 32(e)(u,u,u).

Temperature (°)	25	140	300	420[a]	480[a]	650[a]
a (Å)	9.8848(6)	9.8911(6)	9.9024(6)	9.9143(5)	9.9174(5)	9.9279(8)
u	0.2592(4)	0.2589(4)	0.2588(5)	0.2585(5)	0.2569(2)	0.254(2)
B (Å^2)	1.2(2)	1.4(2)	2.0(2)	2.59(9)	2.83(8)	3.5(3)
A-S (Å)	2.298(6)	2.293(8)	2.296(9)	2.292(8)	2.264(4)	2.23(3)
Cr-S (Å)	2.384(3)	2.388(4)	2.391(5)	2.398(4)	2.413(2)	2.44(2)
Cr-Cr (Å)	3.4948(2)	3.4970(2)	3.5011(2)	3.5052(2)	3.5063(1)	3.5100(2)
S-Cr-S (°)	85.6(2)	85.7(2)	85.7(3)	85.9(2)	86.7(1)	87.9(7)
	94.4(2)	94.2(2)	94.3(3)	94.1(2)	93.3(1)	92.1(7)
CdI_2 (%)[b]	0	0	0	0	0	33
R_{wp} (%)	8.3	9.1	9.4	8.0	8.5	8.8
χ^2	1.1	1.0	1.0	1.0	0.9	0.9

[a] Pt refined with Le Bail method.

[b] Weight fraction.

TABLE III. Final refined parameters for $Co_{0.65}Ni_{0.35}Cr_2S_4$ at 0.4 GPa and 750 °C (CdI_2 phase, space group: $P\overline{3}m1$), with refined lattice parameters: $a=3.4416(2)$ Å and $c=5.6150(7)$ Å. The final goodness-of-fit indicators are $R_{wp}=7.1\%$ and $\chi^2=1.0$.

Atom	Site	x	y	z	B (Å^2)	SOF
A	1(a)	0.0	0.0	0.0	3.6(3)	Co 0.33 Ni 0.17
Cr	1(b)	0.0	0.0	0.5	3.6(3)	1.0
S	2(d)	1/3	2/3	0.256(8)	3.6(3)	1.0

Simulations carried out for both structures in the 35° bank (long d spacings) demonstrated that in the CdI_2 structure the (001) reflection ($d=5.61$ Å), which is forbidden in the $P6_3/mmc$ space group, should have a measurable intensity. Examination of the data collected in the 35° bank for $Co_{0.65}Ni_{0.35}Cr_2S_4$ revealed the existence of a weak peak at $d\approx5.6$ Å and therefore the structure of the high-pressure and high-temperature phase can be identified as being of the CdI_2 type. Final refined parameters for data collected at 750 °C are given in Table III. The CdI_2 phase has a nearly ideal value of the axial ratio c/a, which ensures the maximum packing efficiency. Rietveld refinement using data collected after cooling the sample to room temperature was initiated in the space group $I2/m$ using structural parameters determined for $NiCr_2S_4$.[18] Final refined parameters are shown in Table IV. Representative final observed, calculated and difference profiles for the three observed phases are given in Fig. 3.

$Co_{0.65}Ni_{0.35}Cr_2S_4$ exhibits contrasting magnetic properties in the spinel and Cr_3S_4 forms (Fig. 4). The thiospinel shows a large increase in the magnetization below 240 K, indicative of the onset of long-range magnetic order, whereas the magnetization of the Cr_3S_4-type material is almost independent of temperature. Close examination of the data from the latter, reveal a weak feature at ca. 240 K, consistent with the presence of a small amount of spinel-type material.

C. High-pressure study on $CoCr_2S_4$

Data were collected, at room temperature, at ambient pressure, 5.0, 6.8, and 8.6 GPa. Over the pressure range $0<P/\text{GPa}\leqslant6.8$, the spinel phase remains, but with increasing pressure, the reflections broaden, and at 6.8 GPa additional very broad and weak peaks appear in the diffraction pattern, which could not be indexed on the basis of a NiAs-type phase. At the highest pressure (8.6 GPa), the peaks arising from the spinel phase disappear and only reflections corresponding to the new phase remain, together with some re-

TABLE IV. Final refined atomic parameters for $Co_{0.65}Ni_{0.35}Cr_2S_4$ at 0.4 GPa after cooling to room temperature. The refinement was carried out in the space group $I2/m$ (Cr_3S_4 structure). The final goodness-of-fit indicators are $R_{wp}=7.7\%$ and $\chi^2=1.2$, with final refined lattice parameters $a=5.8946(9)$ Å, $b=3.4063(5)$ Å, $c=11.039(2)$ Å, and $\beta=90.99(1)°$.

Atom	Site	x	y	z	B (Å^2)	SOF
A	2(a)	0.0	0.0	0.0	0.9(2)	Co 0.65 Ni 0.35
Cr	4(i)	−0.021(1)	0.0	0.2549(9)	0.9(2)	1.0
S(1)	4(i)	0.341(2)	0.0	0.358(1)	0.9(2)	1.0
S(2)	4(i)	0.326(2)	0.0	0.885(1)	0.9(2)	1.0

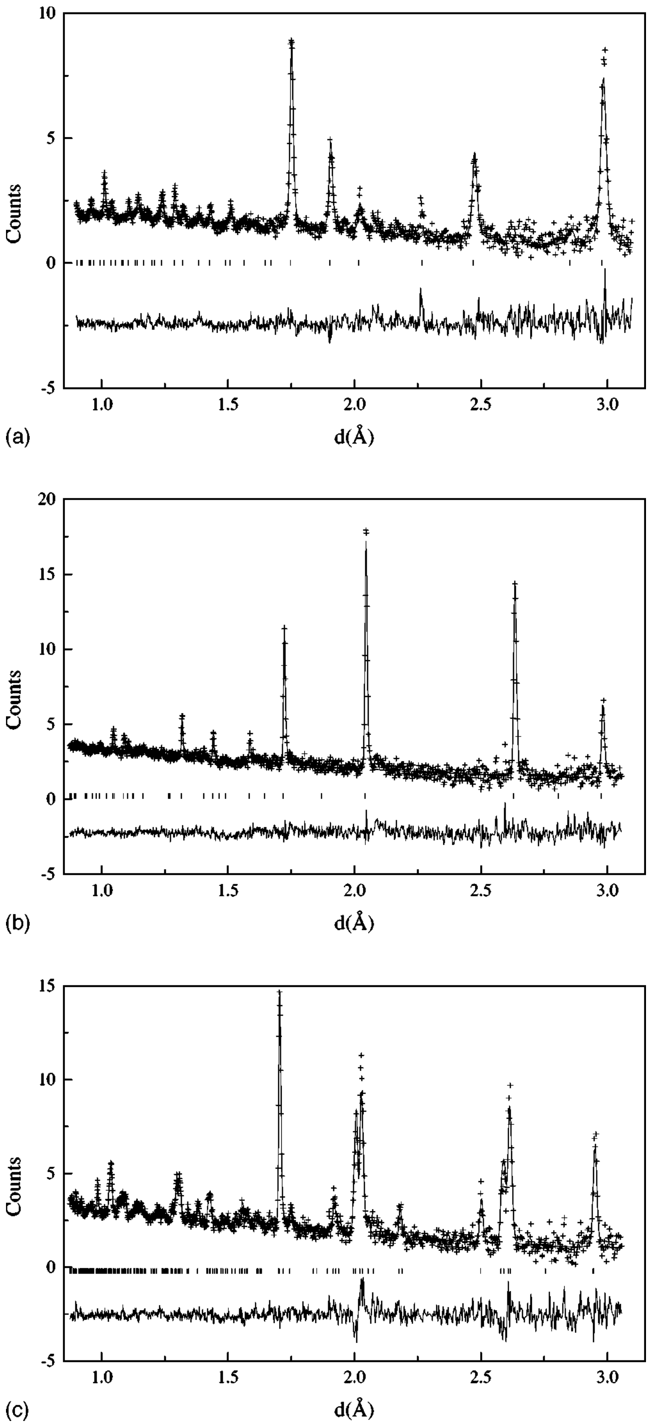

FIG. 3. Observed (crosses), calculated (upper full line), and difference (lower full line) powder neutron-diffraction profiles for $Co_{0.65}Ni_{0.35}Cr_2S_4$ at 0.4 GPa and (a) 140 °C (spinel) (b) 750 °C (CdI_2) (c) after cooling to 25 °C (Cr_3S_4). Reflection positions are marked.

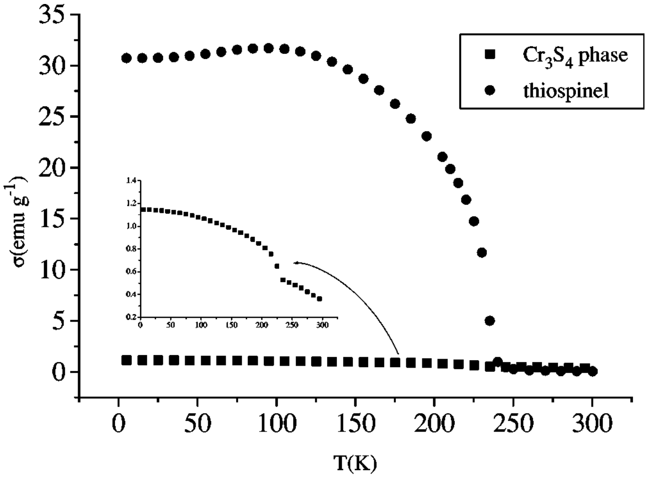

FIG. 4. Temperature dependence of the field-cooled magnetization per gram for $Co_{0.65}Ni_{0.35}Cr_2S_4$ with the spinel and with the Cr_3S_4 structures.

flections of instrumental origin. In Table V the observed reflections at 8.6 GPa are given. Although these reflections could be indexed on the basis of a primitive cubic cell with $a = 4.97(2)$ Å, attempts to solve the high-pressure structure have failed. A single-crystal x-ray-diffraction study on a similar sulphide, the $ZnCr_2S_4$ spinel, reported that this material becomes amorphous under high pressure and that the broadening of the reflections made impossible the collection of data above 8 GPa.[19] Furthermore, it has been shown that at 7.7 GPa the pressure dependence of the resistivity of $CoCr_2S_4$ changes, which suggests a structural transformation.[20] The transformation pressure obtained from conductivity measurements is in agreement with that determined in this work. Release of the pressure resulted in a reversible transformation to the spinel phase.

Rietveld refinements using the data collected below 8.6 GPa were initiated with the structural parameters determined for $CoCr_2S_4$ at room temperature and ambient pressure. Selected final refined parameters, bond lengths, and angles are presented in Table VI. With increasing pressure, the lattice parameter of the spinel decreases, while the positional parameter u increases, which indicates the octahedra are becoming increasingly distorted. This distortion is accompanied by a decrease in the Cr-Cr and Cr-S distances, while the Co-S distances increase slightly. Consequently, whereas the volume of the octahedra decreases by $>11\%$, the volume of the tetrahedra increases by ca. 4% with increasing pressure.

TABLE V. Observed and calculated d-values for the high pressure phase of $CoCr_2S_4$ at 8.6 GPa.

Observed d (Å)	Calculated d (Å)	hkl
2.50	2.48	200
2.26	2.22	210
1.77	1.76	220
1.57	1.57	310
1.32	1.33	321

TABLE VI. Final refined parameters, selected bonds and angles for the spinel $CoCr_2S_4$ at room temperature as a function of pressure.

Pressure (GPa)	10^{-4}	5.0	6.8
a (Å)	9.8985(4)	9.7634(8)	9.703(2)
u	0.2574(4)	0.2595(4)	0.2618(7)
Volume (Å^3)	969.8(1)	930.6(2)	913(5)
Co-S (Å)	2.270(6)	2.274(7)	2.30(1)
Cr-S (Å)	2.404(3)	2.352(4)	2.317(6)
Cr-Cr (Å)	3.4996(1)	3.4519(2)	3.4306(4)
S-Cr-S (°)	86.5(2)	85.4(2)	84.2(4)
	93.5(2)	94.6(2)	95.8(4)
R_{wp}	7.4	7.0	8.2
χ^2	1.2	1.5	1.4

IV. DISCUSSION

The thiospinel $CoCr_2S_4$ transforms to a defect NiAs-type phase at 1.3 GPa and 800 °C. However, replacement of 35% of the cobalt ions with nickel, causes a dramatic decrease, by a factor of 3, in the transformation pressure and $Co_{0.65}Ni_{0.35}Cr_2S_4$ undergoes this phase change at 0.4 GPa and 750 °C. In both cases, the structural transition is accompanied by a decrease in volume of ca. 7%, which is comparable to those reported in the literature for ACr_2S_4 (A = Mn, Fe, Co).[7] The discontinuity in volume, and the coexistence of two phases over a temperature range, suggest that the phase transition is of first order. Moreover, comparison of the transformation pressure of $CoCr_2S_4$ with that of $Co_{0.65}Ni_{0.35}Cr_2S_4$ shows that the strong preference of Ni^{2+} for the octahedral sites,[21] combined with the strong octahedral preference of Cr^{3+}, causes a stabilization of the cation-deficient NiAs structure, which contains only octahedral cation sites.

The P-T diagram proposed by Albers and Rooymans[5] for the thiospinels should be modified to include a new phase region at low temperature and very high pressure. This new phase appears to be cubic, but its structure remains unknown. AB_2S_4 materials with large A and B ions adopt the Th_3P_4 or the CaY_2S_4 structures, and therefore $CoCr_2S_4$ might be expected to adopt one or other of these structures at very high pressures. However, attempts to model the high-pressure data with either of these structures, with a variety of rocksalt superstructures, including $LiFeO_2$ or α-$NaFeO_2$, or distorted spinels, were unsuccessful. The broadening of the peaks and the marked decrease in intensity observed for $CoCr_2S_4$ under pressure suggest that the structure is becoming increasingly disordered. In many cases it has been observed that, at room temperature, materials under high pressure may amorphize due to the absence of the thermal activation required to increase the coordination number.[22] Moreover, pressure-induced transformations of ternary oxides and chalcogenides ABX_2 at low temperatures give rise to disordered high-pressure modifications, where the A and B cations are disordered in the lattice, while the transformation at higher temperatures can give rise to an ordered structure.[8]

For $Co_{0.65}Ni_{0.35}Cr_2S_4$, cooling of the high-pressure phase (disordered NiAs-type structure) to room temperature resulted in a transition to a Cr_3S_4 phase, due to the ordering of the metal vacancies in every second layer. There is considerable confusion in the literature concerning the results obtained with quenched materials, such as $FeCr_2S_4$. In some cases a disordered NiAs-type phase has been observed, while at other times an ordered NiAs-type phase (Cr_3S_4) was reported.[7,8] The results presented in this work suggest that the disordered NiAs-type phase is stable only at high temperatures. This has been previously observed in many other systems, in which the NiAs-type phase is a high-temperature phase, being rarely retained in equilibrium conditions at low temperatures[4] where superstructures (such as Cr_3S_4),[23] or distorted structures (such as MnP),[24] frequently occur.

In the cobalt chromium thiospinel the Co^{2+} and Cr^{3+} sublattices are aligned antiparallel since the A-Cr interaction is much stronger than the A-A or Cr-Cr interactions.[25] This gives rise to ferrimagnetic behavior. The behavior of the thiospinel $Co_{0.65}Ni_{0.35}Cr_2S_4$ is similar, with a slightly higher magnetic ordering temperature ($T_C = 240$ K).[12] In contrast to this, the Cr_3S_4 phase of $Co_{0.65}Ni_{0.35}Cr_2S_4$ exhibits a very low magnetization which is almost temperature independent. Comparison of these magnetic data with those of Cr_3S_4 phases stable at ambient conditions, show that, however, the curves are quite different. As reported previously by Tressler and Stubican,[11] it is quite difficult to maintain quenched ACr_2S_4 materials with the Cr_3S_4 structure at ambient pressure, and the materials usually contain a small amount of spinel ($<5\%$). This seems to be the case with $Co_{0.65}Ni_{0.35}Cr_2S_4$, thus the magnetization curve is the sum of the contributions of the two phases. As the magnetization for Cr_3S_4 phases is very weak and almost temperature independent, owing to a complex magnetic structure with predominant antiferromagnetic interactions,[18] even a small contribution from the strongly ferrimagnetic spinel is sufficient to mask the behavior of the Cr_3S_4 phase.

ACKNOWLEDGMENTS

We wish to thank the EPRSC for a research grant in support of our neutron scattering program. One of the authors (P.V.) thanks The Leverhulme Trust for financial support.

---

[1] R. P. van Stapele, in *Ferromagnetic Materials*, edited by E. P. Wohlfarth (North-Holland, Amsterdam, 1982), Vol. 3.

[2] C. N. Rao and K. P. R. Pidharody, Prog. Solid State Chem. **10**, 207 (1979).

[3] H. D. Megaw, *Crystal Structures: A Working Approach* (W. B. Saunders Company, Philadelphia, 1973).

[4] A. Kjekshus and W. B. Pearson, Prog. Solid State Chem. **1**, 83 (1964).

[5] W. Albers and C. J. M. Roymans, Solid State Commun. **3**, 417 (1965).

[6] R. E. Tressler, F. A. Hummel, and V. S. Stubican, J. Am. Ceram. Soc. **51**, 648 (1968).

[7] R. J. Bouchard, Mater. Res. Bull. **2**, 459 (1967).

[8] C. J. M. Rooymans, Philips Res. Rep. Suppl., No. 5 (1968).

[9] P. Vaqueiro, S. Hull, B. Lebech, and A. V. Powell, J. Mater. Chem. **9**, 2859 (1999).

[10] W. Albers, G. van Aller, and C. Haas, *Propriétés Thermodynamiques Physiques et Structurales des Dérivés Semi-Metalliques* (CNRS, Paris, 1967).

[11] R. E. Tressler and V. S. Stubican, J. Am. Ceram. Soc. **51**, 391 (1968).

[12] P. Vaqueiro, S. Sommer, and A. V. Powell, J. Mater. Chem. **10**, 2381 (2000).

[13] S. Hull, D. A. Keen, R. Done, T. Pike, and N. J. G. Gardner, Nucl. Instrum. Methods Phys. Res. A **385**, 354 (1997).

[14] J. M. Besson, R. J. Nelmes, G. Hamel, G. Weill, J. S. Loveday, and S. Hull, Physica B **180+181**, 907 (1992).

[15] W. I. F. David, M. W. Johnson, K. J. Knowles, C. M. Moreton-Smith, G. D. Crisbie, E. P. Campbell, S. P. Graham, and J. S. Lyall, Rutherford Appleton Laboratory, Report No. RAL-86-102, 1986.

[16] A. C. Larson and R. B. von Dreele, General Structure Analysis System, Los Alamos Laboratory, Report No. LAUR 85-758, 1994.

[17] R. B. von Dreele, High Press. Res. **14**, 321 (1996).

[18] A. V. Powell, D. C. Colgan, and C. Ritter, J. Solid State Chem. **134**, 110 (1997).

[19] J. Wittlinger, S. Werner, and H. Schultz, Phys. Chem. Miner. **24**, 597 (1997).

[20] V. F. Skume, E. S. Polulyak, M. R. Allazov, E. F. Zhukov, A. S. Skoropanov, A. Vecher, and V. A. Fedorov, Inorg. Mater. **23**, 1537 (1987) (Transl. of Izv. Akad. Nauk SSSR, Neorg. Mater.).

[21] A. Miller, J. Appl. Phys. **30**, 24S (1959).

[22] C. M. Edwards, J. Haines, I. S. Butler, and J-M. Léger, J. Phys. Chem. Solids **60**, 529 (1999).

[23] F. Jellinek, Acta Crystallogr. **10**, 620 (1957).

[24] W. Tremel, R. Hoffmann, and J. Silvestre, J. Am. Chem. Soc. **108**, 5174 (1986).

[25] P. Gilbart, J. L. Dormann, and Y. Pellerin, Phys. Status Solidi **36**, 187 (1969).